Mathematics Today Vol.33 (June & December 2017) 75-87
ISSN 0976-3228, E-ISSN 2455-9601

# Homotopy Solution for Magnetohydrodynamic 3-D Flow of Nanofluid over a Shrinking Sheet in the Presence of Thermal Radiation

Shankar Rao Munjam[1] and Ram Prakash Sharma*[2]

[1]School of Naval Architecture, Ocean and Civil Engineering,
Shanghai Jiao Tong University, Shanghai, 200240, China
[1] Email: munjam@sjtu.edu.cn

[2]Department of Mathematics, JECRC University,
Jaipur 303-905, Rajasthan, India
[2] Email: ramprakash0808@gmail.com

***Corresponding author**: Ram Prakash Sharma

## Abstract

This article aims to investigate the 3D magetohydrodynamic (MHD) flow of viscous nanofluid past saturating porous medium in the presence of thermal radiation. The flow is induced by a convectively heated permeable shrinking sheet. The arising system of nonlinear partial differential equations are converted to ordinary differential equations. Flow and heat transfer properties are evaluated by homotopy Analysis. The outcomes of velocity, temperature and Nusselt number are studied for various parameters of interest. It is found that temperature is enhanced with an enhancement in the radiation parameter and higher nanoparticle volume fraction reduces the velocity field. Also the temperature and Nusselt number are increased for greater values of Biot number.

**Keywords:** Thermal radiation; MHD; Nanofluid; Shrinking sheet; Porous medium; Convective boundary conditions.
**2000 AMS subject classification code:** 31B35, 34-02, 35G30, 35Q35, 76S05, 76W05.

## Introduction:

In recent years, the flow analysis of nanofluids has been the topic of extensive research because of its properties in increasing thermal conductivity in heat transfer process. Many ordinary fluids, including water, toluene, ethylene glycol and mineral oils, etc., in heat transfer processes have rather low thermal conductivity. The nanofluid is an advanced type of fluid containing nanometer-sized particle having diameter less than 100 nm or fibbers suspended in the ordinary fluid. Initially nanofluid introduced by Choi [1]. The research on heat transfer in nanofluids has been receiving increased attention worldwide.

Several researchers have obtained unexpected thermal characteristics of nanofluids and have given new mechanism behind the increased thermal properties of nanofluids. Das *et al.* [2] in their book entitled "Nanofluids: Science and Technology" have given details and methodologies of convective heat transfer in nanofluids. The nanoparticles are quite significant even in natural phenomena through over a broad spectrum of science and engineering disciplines, especially in the field of chemical engineering. Nanofluids remarkably enhance the thermal conductivity of a conventional liquid, which is beyond the description of any existing

methods. Nanofluids are stable and free from extra issues of sedimentation, additional pressure drops, rheological and Erosion characteristics.

In view of these applications of nanofluids, several researchers have been investigated the various cases in nanofluid [3-5]. Kakac *et al.* [6] have investigated the convective heat transfer enhancement with nanofluids.The slip flow and heat transfer of a non-Newtonian nanofluid due to a micro tube has been analyzed by Niu *et al.* [7]. Xu *et al.* [8] have examined the flow and heat transfer in a nano-liquid film over an unsteady stretching surface. Turkyilmazoglu [9] has been studied nanofluid flow and heat transfer in a rotating disk. The heat transfer effects in a nanofluid flow over a permeable stretching wall in a porous medium and the rotating system over a magnetic field, and also investigated in MHD nanofluid flow and heat transfer by means of two phase models has been analyzed by Sheikholeslami et al. [10-12]. A steady 3-dimensional MHD flow of couple stress nanofluid over a shrinking sheet with viscous dissipation and Joule heating through porous medium has been discussed by Ramzan [13]. The convective conditions on MHD 3-dimensional flow of nanofluid have been considered by Hayat *et al.* [14]. Hady *et al.* [15] have presented the effects of radiation on viscous flow of a nanofluid and heat transfer over a nonlinearly stretching sheet. Thermal radiation effects on the MHD boundary layer flow of a nanofluid past a stretching sheet with convective boundary conditions and also considered nanofluid past a porous shrinking sheet has been studied by Nadeem *et al.* [16-17].

The study of convection flow of nanofluids with heat and mass transfer over a vertical infinite flat plate, in the presence of magnetic field and radiation has important applications in various chemical and engineering processes such as petroleum and chemical industry, cooling of nuclear reactors and thermal insulation. Turkyilmazoglu *et al.* [18] have examined the heat and mass transfer of unsteady natural convection flow of some nanofluids past a vertical infinite flat plate with radiation effect. The nanofluid flow with multimedia physical features for conjugate mixed convection and radiation effects has been analyzed by Hsiao [19]. Kahar *et al.* [20] have investigated the scaling group transformation for boundary-layer flow of a nanofluid past a porous vertical stretching surface in the presence of chemical reaction with radiation effects. The HAM method is described in detail in [21], it is not explained here for the sake of brevity.

Rauf *et al.* [22] have investigated the magnetohydrodynamic stagnation point flow of a nanofluid by a shrinking surface in the presence of first order chemical reaction. Priyadarsan *et al.* [23] have studied the heat transfer influence on MHD 3D flow of nanofluid by a shrinking sheet with viscous dissipation and thermal radiation. They analyzed the series solution by employing HAM. They obtained that magnetic field impedes the fluid motion leading to thinner momentum boundary layer and enhancement in thermal radiation as well as viscous dissipation reduces the heat transfer rate from the shrinking sheet. 3D free convective MHD flow of nanofluid over permeable linear stretching sheet with thermal radiation has been studied by Nayak *et al.* [24]. They found that the presence of magnetic field slows down the fluid motion while it enhances the fluid temperature leading to a reduction in heat transfer rate from the surface. They also found that enhancing thermal radiation parameter causes a reduction in heat transfer rate.

Effect of thermal radiation on MHD mixed convective heat transfer adjacent to a vertical continuously stretching sheet in the presence of variable viscosity described by Salem *et al.* [25]. Raptis *et al.* [26] have

studied Radiation and free convection flow through a Porous medium. MHD flow and heat transfer over a porous shrinking surface with velocity slip and temperature jump has been illustrated by Zheng *et al.* [27].

All these studies were either numerical methods or semi-analytical techniques on stretching surface for various cases of flow are available in the literature [9-15, 21]. Since the approximate analytical solution for the magnetohydrodynamic (MHD) 3-dimensional flow of nanofluid over a shrinking sheet with thermal radiation through porous medium which has not been taken up for analysis in [14]. The focus of this research work is to investigate the HAM solution for MHD 3D flow of nanofluid past a shrinking sheet with thermal radiation through porous medium.

**Mathematical Formulation:**

We consider a steady 3-D flow of an incompressible nanofluid past a shrinking sheet under the influence of thermal radiation through porous medium. A uniform transverse magnetic field $B_0$ is applied parallel to z-axis and shown in Fig.1. It is also assumed that the induced magnetic and electric fields are neglected. The convective boundary conditions are retained in the heat transfer procedure.

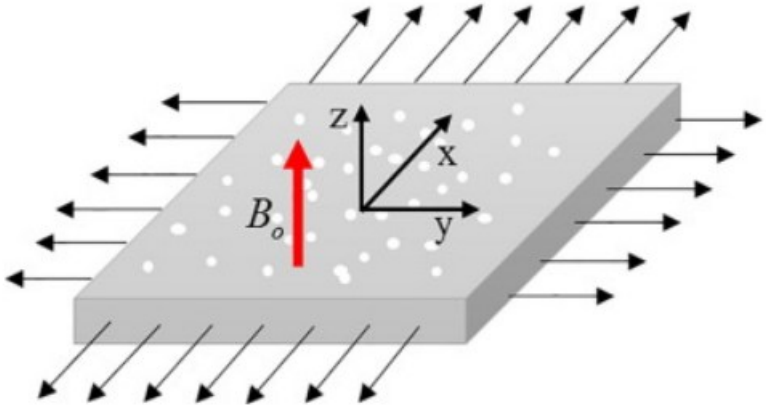


Fig. 1. Schematic diagram of 3-D stretching sheet under the effects of magnetic field.

The governing equations [14] are given by

$$\frac{\partial u}{\partial x}+\frac{\partial v}{\partial y}+\frac{\partial w}{\partial z}=0 \tag{1}$$

$$u\frac{\partial u}{\partial x}+v\frac{\partial u}{\partial y}+w\frac{\partial u}{\partial z}=\nu_{nf}\frac{\partial^2 u}{\partial z^2}-\frac{\sigma {B_0}^2 u}{\rho_{nf}}-\frac{\nu_{nf}}{K}u \tag{2}$$

$$u\frac{\partial v}{\partial x}+v\frac{\partial v}{\partial y}+w\frac{\partial v}{\partial z}=\nu_{nf}\frac{\partial^2 v}{\partial z^2}-\frac{\sigma {B_0}^2 v}{\rho_{nf}}-\frac{\nu_{nf}}{K}v \tag{3}$$

$$u\frac{\partial T}{\partial x}+v\frac{\partial T}{\partial y}+w\frac{\partial T}{\partial z}=\alpha_{nf}\frac{\partial^2 T}{\partial z^2}-\frac{1}{(\rho C_p)_{nf}}\frac{\partial q_r}{\partial z}, \tag{4}$$

The boundary conditions for the considered flow analysis are

$$u = bx, v = b(m-1)y, w = -W, -k_f \frac{\partial T}{\partial z} = h(T_f - T) \ \ at\, z = 0, \tag{5}$$

$$u \to 0, v \to 0, T \to T_\infty \ \ as\, z \to \infty, \tag{6}$$

where $u, v$ and $w$ are the velocity components of the nanofluid along the $x-, y-$ and $z-$ directions respectively. $\sigma$ Indicates the electrical conductivity of fluid and K denotes the permeability of porous medium. W is the suction velocity, b < 0 denotes shrinking constant and h bex` the convective heat transfer coefficient. $k_{nf}$ and $\alpha_{nf}$ denotes the thermal conductivity and the thermal diffusivity respectively, and $\rho_{nf}$ and $\mu_{nf}$ indicates the effective density and the effective dynamic viscosity, and $(\rho C_p)_{nf}$ be the heat capacitance and the thermal conductivity $k_{nf}$ of the nanofluid [17], which are given by

$$\alpha_{nf} = \frac{k_{nf}}{(\rho C_p)_{nf}}, \tag{7}$$

$$\rho_{nf} = \rho_f (1-\phi) + \rho_s \phi, \tag{8}$$

$$\mu_{nf} = \frac{\mu_f}{(1-\phi)^{2.5}}, \tag{9}$$

$$(\rho C_p)_{nf} = (\rho C_p)_f (1-\phi) + (\rho C_p)_s \phi, \tag{10}$$

$$\nu_{nf} = \frac{k_{nf}}{k_f}, \tag{11a}$$

The nanoparticle volume fraction ϕ denoted as

$$\phi = \frac{\rho_{nf} - \rho_f \rho_s}{\rho_s - \rho_f} \tag{11b}$$

The magnetic field $B_0$ for the flow defined as

$$B_0 = \frac{B}{\sqrt{1-m}}. \tag{11c}$$

We noticed that the magnetic moment m**,** when m =1, the sheet shrinks in x-direction only and the sheet shrinks axis symmetrically for m =2. B is a constant, where $\rho_f$ and $\rho_s$ are the densities of the base fluid and nanoparticle respectively, suffix s is denoted the nanofluid supplied in weight concentration, $(\rho C_p)_f$ and $(\rho C_p)_s$ indicates the specific heat parameters of the base fluid and nanoparticle respectively, $\mu_f$ denotes the viscosity of the base fluid, and $k_f$ and $k_s$ are the thermal conductivities of the base fluid and nanoparticle respectively.

Using the Roseland approximation [25, 26] for radiation, the radiative heat flux $q_r$ is simplified as

$$q_r = -\frac{4\sigma^*}{3k^*}\frac{\partial T^4}{\partial z} \tag{12}$$

where $\sigma^*$ and $k^*$ are the Stefan-Boltzman constant and the mean absorption coefficient, respectively. We assume that the temperature differences within the flow are such that the term $T^4$ may be expressed as a linear function of temperature. Hence, expanding $T^4$ in a Taylor series about $T_\infty$ and neglecting higher order terms we get

$$T^4 \cong 4T_\infty{}^3 T - 3T_\infty{}^4 \tag{13}$$

Using (12) and (13) in the Energy equation (4) we obtain

$$u\frac{\partial T}{\partial x} + v\frac{\partial T}{\partial y} + w\frac{\partial T}{\partial z} = \alpha_{nf}\left(\frac{3N_R + 4}{3N_R}\right)\frac{\partial^2 T}{\partial z^2} \tag{14}$$

where $N_R = \dfrac{k_{nf}k^*}{4\sigma^* T_\infty{}^3}$ is the radiation parameter.

Introducing [14]:

$$\eta = \sqrt{\frac{a}{\nu_f}}\, z, u = a\,x\,f'(\eta), v = a\,(m-1)y\,f'(\eta), w = -\sqrt{a\nu_f}\; m\,f(\eta), G(\eta) = \frac{T - T_\infty}{T_f - T_\infty} \tag{15}$$

Equation (1) is satisfied automatically and equations (2)–(4) are become

$$\varepsilon_1 f''' + m\,f\,f'' - f'^2 - M\varepsilon_1(1-\phi)^{2.5} f' - \Pr\, d\varepsilon_1 f' = 0 \tag{16}$$

$$\left(\frac{3N_R + 4}{3N_R}\right)\frac{A_1}{\Pr}(1-\varphi)^{2.5}\,\varepsilon_2 G'' + m\,fG' = 0\,. \tag{17}$$

with the boundary conditions

$$f(0) = S, f'(0) = \lambda, G'(0) = -\gamma[1 - G(0)],\; f'(\infty) = 0, G(\infty) = 0. \tag{18}$$

here f is the dimensionless stream function; $f'$ is the dimensionless velocity and G is the dimensionless temperature, respectively. $S = \dfrac{W}{\sqrt{a\nu_f}\,m}$ indicates the mass transfer parameter (S >0 for suction and S < 0 for injection). $M = \dfrac{\sigma B_0{}^2}{\rho_f\, a}$ be the Hartman number, Where a > 0, $d = \dfrac{\alpha_f}{aK}$ be the porosity parameter, $\Pr = \dfrac{\nu_f\,(\rho C_p)_f}{k_f}$ denotes the Prandtl number, $\lambda = b/a$ denotes the shrinking parameter, $\gamma = \dfrac{h}{k}\sqrt{\dfrac{\nu}{a}}$ indicates the Biot number, and $\varepsilon_1, \varepsilon_2$ and $A_1$ are constant relating to the characteristics of nanofluid described below: $\varepsilon_1 = \dfrac{1}{(1-\phi)^{2.5}\left[1 - \phi + \phi\dfrac{\rho_s}{\rho_f}\right]}$ (19)

$$\varepsilon_2 = \frac{1}{(1-\varphi)^{2.5}\left[1-\varphi+\varphi\frac{(\rho C)_s}{(\rho C)_f}\right]} \tag{20}$$

$$A_1 = \frac{k_s + 2k_f - 2\phi(k_f - k_s)}{k_s + 2k_f + \phi(k_f - k_s)}, \tag{21}$$

And the local Nusselt number $Nu$ define as

$$Nu = \frac{x\, q_w}{k_f (T_f - T_\infty)} \text{ where the surface heat flux } q_w \text{ contents} \tag{22}$$

$$q_w = k_{nf}\left.\frac{\partial T}{\partial z}\right|_{z=0} \tag{23}$$

by using Eqs. (17) and (23), we have

$$Nu(\mathrm{Re}_x)^{-\frac{1}{2}} = A_1 G'(0) \tag{24}$$

where $\mathrm{Re}_x = \frac{u_w x}{\nu_f}$ indicates the local Reynolds number.

**Solution Methodology:**

The recently developed approximate analytical method is applied to obtain the desired solutions. In homotopy analysis, we usually get a system of differential equations which have to be solved. We present the detailed analysis of the advanced HAM to solve our coupled nonlinear partial differential equations (i.e. Eqs. (16)-(17)) with the boundary conditions (18). The appropriate initial approximations such as base function, initial guesses and auxiliary linear operators as follows;

$$\{(\eta^m e^{-n\eta}),\ m \geq 0,\ n \geq 0\},\ X(\eta) = A^0_{0,0} + \sum_{n=0}^{\infty}(A^m_{\ell,n}\eta^m e^{-n\eta}), \tag{25}$$

where X = f and G; $A^m_{l,n}$ is the coefficient to be determined. Let

$$f_0(\eta) = 1 - e^{-\eta},\ G_0(\eta) = e^{-\eta};\ L_f = f''' - f';\ L_G = G'' - G. \tag{26}$$

so as to obtain a simpler form of solution as

$$L_f[\mathbf{C_1} + \mathbf{C_2}e^{\eta} + \mathbf{C_3}e^{-\eta}] = 0;\ L_G[\mathbf{C_4}e^{\eta} + \mathbf{C_5}e^{-\eta}] = 0 \tag{27}$$

here Ci's (i=1, 2,…) are arbitrary constants and can be obtained from Eq. (18).

After rigorous analysis, we get a system of differential equations called deformation equations which have to be solved up to a desired order.

**Deformation Equations:**

To obtain the solution for Eqs. (16) - (17), when $\gamma \in [0, 1]$ and $c_f$, $c_G$ be are the convergence control parameters (CCP). Then the non-linear operators and zeroth and $l^{\text{th}}$-order deformation equations take the form as explained in [21]. Thus $\gamma$ increases from 0 to 1 and $f(\eta, \gamma)$, $G(\eta, \gamma)$ varies from the initial guess $f_0(\eta)$ and $G_0(\eta)$ to the solution $f(\eta)$ and $G(\eta)$ of (16) and (17), respectively. So that the solution series converges when $\gamma = 1$ as,

$f(\eta) = f_0(\eta) + \sum_{l=1}^{\infty}[f_l(\eta)]$ and $G(\eta) = G_0(\eta) + \sum_{l=1}^{\infty}[G_l(\eta)]$. (28)

Clearly, the general solution $f_l$ and $G_l$ in terms of special solutions $f_l^*$ and $G_l^*$ are given by

$f_l(\eta) = f_l^*(\eta) + \mathbf{C}_1 + \mathbf{C}_2 e^{\eta} + \mathbf{C}_3 e^{-\eta}$ and $G_l(\eta) = g_l^*(\eta) + \mathbf{C}_4 e^{\eta} + \mathbf{C}_5 e^{-\eta}$. (29) We solve the Eq. (29) by using the orders $l = 1, 2, 3, \ldots\ldots\ldots$ with computational software's Maple and Mathematica 10.0. The solution is always represented as a series solution as a polynomial. Though the computations have been performed up to high order, the results are presented here for the velocity and temperature profiles evaluated up to six terms in the series.

**Error analysis on High orders:**

In order to choose CCP's $c_f$ and $c_G$, we have presented the average squared residual Errors (ASRE) as [21],

$\mathbf{E}_X \approx \frac{1}{\ell}\sum_{j=0}^{i}\left[N\left(\sum_{i=0}^{\ell} X_i(j\Delta x)\right)\right]^2$, here $\Delta x = 10/\ell$ and $\ell = 30$. (30)

From Eq. (30) to find $c_f$ and $c_G$ values and obtained these values are used for the entire computations of solution. The HAM based Mathematica package BVPh 2.0 has been utilized to compute the average residual errors of (16)-(17).

In all of the figures and table, select the parameters Pr = 7.2, $N_R = 0.5$, $\gamma = \phi = 0.1$, $d = M = 0.2$, $\lambda = -0.1$, $\mathrm{m} = 2.0$ and $S = 0.5$ unless it is mentioned otherwise.

Table1. Convergence of homotopy solution for different orders of approximation for $-f''(0)$ and $-G'(0)$ when $d = M = 0.2$, $\gamma = \phi = 0.1$, $S = 0.5$, $m = 2$, $\lambda = -0.1$, $N_R = 0.5$ and $\mathrm{Pr} = 7.2$.

| $l$ | $-f''(0)$ | $-G'(0)$ |
|---|---|---|
| 1 | 1.190276 | 0.686211 |
| 5 | 1.222219 | 0.748503 |
| 10 | 1.259242 | 0.807322 |
| 15 | 1.280033 | 0.820423 |
| 20 | 1.297346 | 0.820423 |
| 25 | 1.297346 | 0.820423 |
| 30 | 1.297346 | 0.820423 |

Table 2. Value of $Nu(\mathrm{Re}_x)^{-\frac{1}{2}}$ results for $-A_1 G'(0)$ when $d = 0.2$, $S = 0.5$, $m = 2$, $\lambda = -0.1$, $N_R = 0.5$ and $\mathrm{Pr} = 7.2$.

| $M$ | $\gamma$ | $\phi$ | $-A_1 G'(0)$ |
|---|---|---|---|
| 0.5 | 0.1 | 0.1 | 0.098621 |
| 1.0 | 0.3 | 0.2 | 0.248503 |
| 1.5 | 0.6 | 0.3 | 0.367322 |
| 2.0 | 0.9 | 0.4 | 0.470057 |

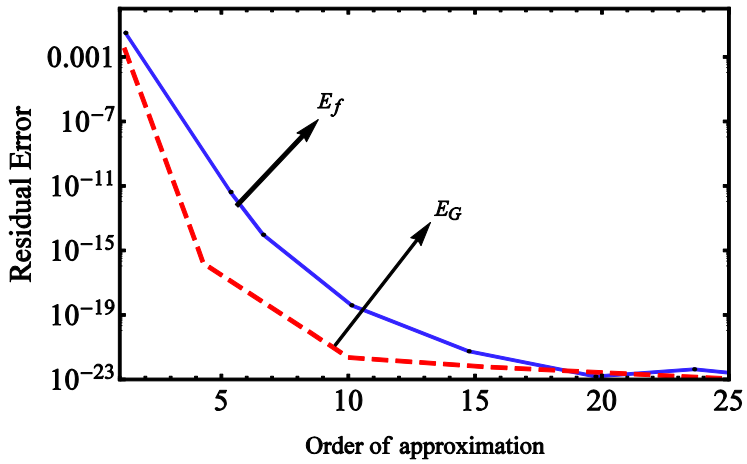


Fig 2. Residual errors v/s order of approximations when $d = 0.2,\ S = 0.5,\ m = 2, \lambda = -0.1,\ N_R = 0.5$ and $\Pr = 7.2$.

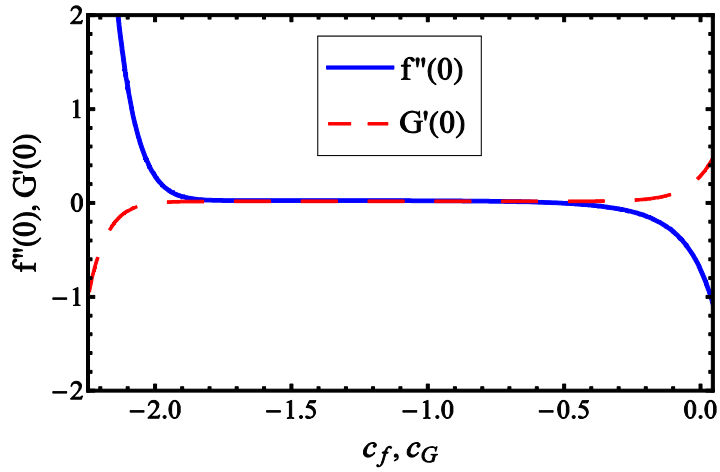


Fig 3. $c_f$, $c_G$-curves for the functions $f''(\eta)$ and $G'(\eta)$ at $\eta = 0$ when $d = 0.2,\ S = 0.5,\ m = 2, \lambda = -0.1,\ N_R = 0.5$ and $\Pr = 7.2$.

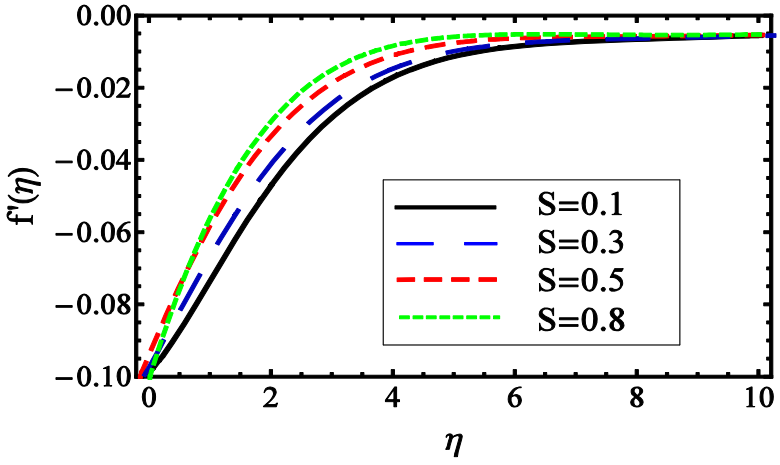


Fig 4. Influence of $S$ on $f'(\eta)$.

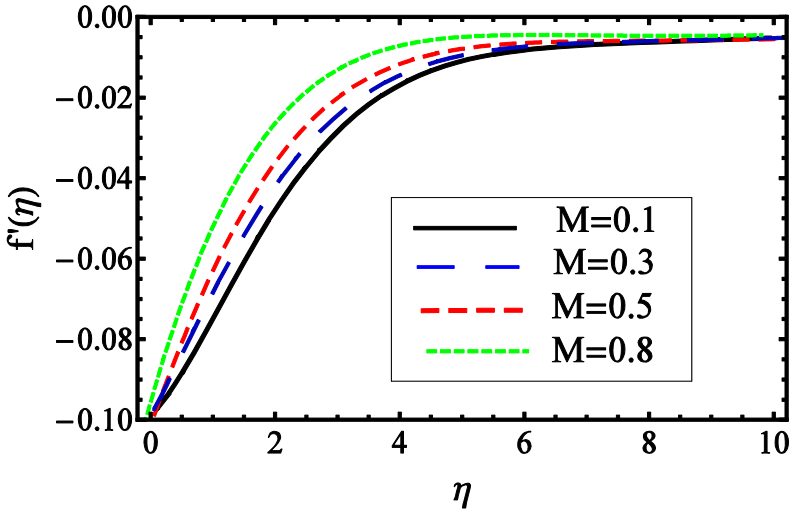


Fig 5. Influence of M on velocity profile.

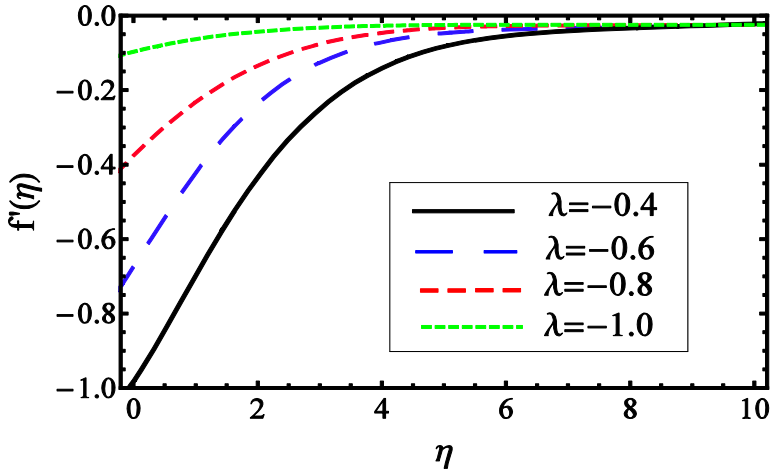


Fig 6. Influence of $\lambda$ on $f'(\eta)$.

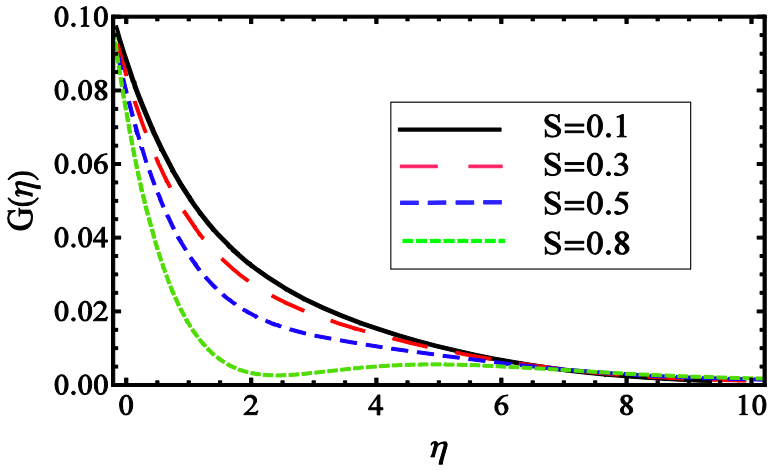


Fig 7. Influence of $S$ on $G(\eta)$.

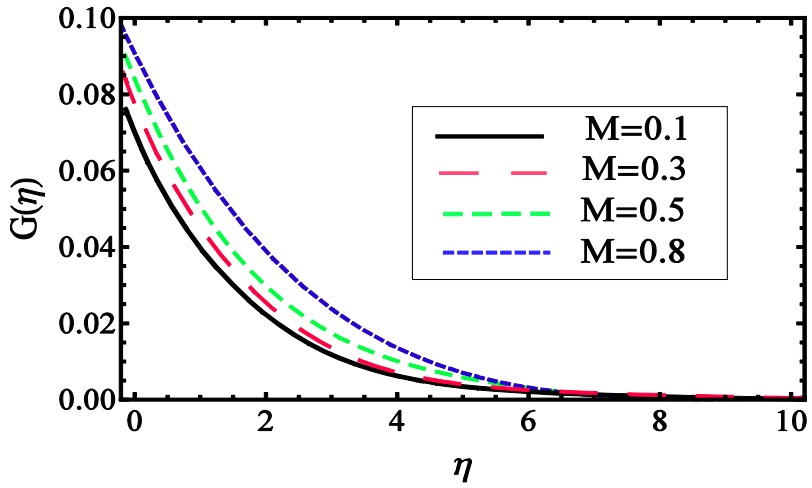


Fig 8. Influence of $M$ on $G(\eta)$.

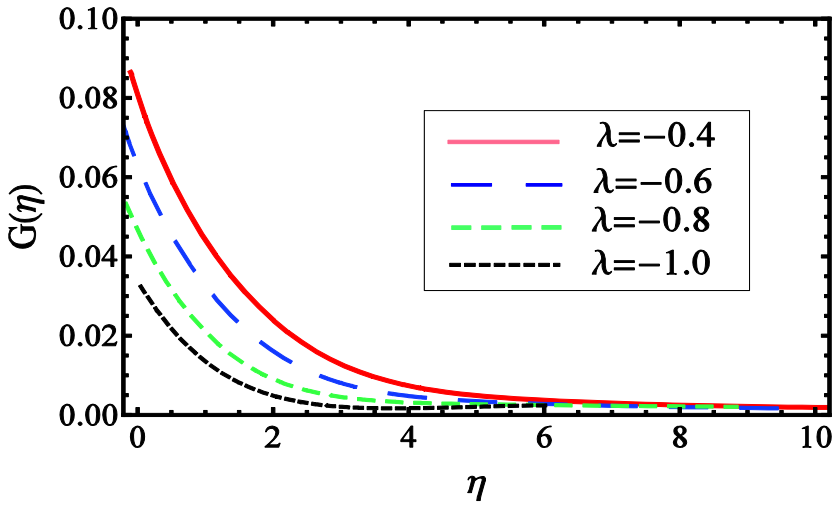


Fig 9. Influence of λ on $G(\eta)$.

**Results and discussion:**

The analytical solutions of velocity and temperature profiles so obtained are a set of polynomials in higher powers of CCP's whose coefficients contain as mass transfer parameter (S), shrinking parameter ($\lambda$) and Hartman number (M) on velocity and temperature profiles. It is found that, velocity and temperature profiles increase with increasing the Hartman number.

Computations have been carried out for velocity and temperature profiles for several combinations of parameters S, M and $\lambda$, only few important and interesting results are reported in this research article in the form of tables and figures. Tables 1–2 and Figures 2-9 presented various results obtained from our analysis.

Tables1 illustrates the convergence of skin friction $-f''(0)$ and heat transfer $-G'(0)$ after performing up to $30^{th}$-order approximation of functions $f$ and $G$ computed from deformation equations. As seen, the computation is terminated as soon as three consecutive values agree in their sixth decimal places. Numerical values of local

Nusselt number for different emerging parameters are presented in Tables 2. It is found that the local Nusselt number $Nu(\mathrm{Re}_x)^{-\frac{1}{2}}$ increases for larger values of Hartman number (M), Biot number (γ) and nanoparticle volume fraction (ϕ).

The average squared residual error $E_X$ at different orders of approximation for $f(\eta)$ and $G(\eta)$ is shown as Fig. 2. The corresponding ASRE decreases very rapidly and we found proper values of the CCP's as $c_f = -1.297346$ and$c_G = -0.820423$. Therefore, the suitable choice of CCP's can greatly accelerate the convergence of series solution in HAM.

It is shown that the solution for the velocity profile can be expressed as an infinite series of any desired order. It is customary in HAM analysis to draw $c_f$ and $c_G$-curves to identify the interval of optimal CCP's inside which any suitable values can be chosen. In Fig. 3 it is shown that choosing unique value from the ranges of $c_f \epsilon [-2.3, -0.5]$ does not affect the values of surface shear stress rates and it is $c_G \epsilon [-2.0, -0.5]$for surface heat transfer rates. Fig. 4 shows the influence of mass transfer parameter S on the velocity profile. It is observed that increasing the S, the magnitude of velocity profile decreases because applying suction leads to draw the amount of fluid particles into the wall and consequently the velocity boundary layer decreases. The effect of Hartman number M on the velocity profile is plotted in Fig. 5 from which it is seen that the magnitude of velocity profile decreases as the M increases. This is because, an applied magnetic field has the tendency to slow down the movement of the fluid, which leads to a decrease in the velocity and momentum boundary layer thickness. Figs.6 presents the effect of shrinking parameter λ on velocity profile. It is observed that the velocity profiles increases when the λ decreases.

The effect of mass transfer S on temperature profile $G(\eta)$ is plotted in Fig. 7. It is observed that the increase in mass transfer makes the temperature profile to converge faster to its free stream values. Fig. 8 gives the temperature profile for various values of Hartman number M. The temperature profile increases for the increase in the values of M. This is due to the fact that, the Lorentz force is a resistive force which opposes the fluid motion. As a sequence heat is produced and hence the thermal boundary layer thickness increases. Fig. 9 presents the effect of shrinking parameter λ on temperature profile $G(\eta)$. It is observed that the temperature profiles decreases when the λ increases.

**Conclusions**

We performed approximate analytical solution for the magnetohydrodynamic (MHD) 3-D flow of nanofluid past a shrinking sheet under the influence of thermal radiation effects investigated by using the homotopy analysis method and profiling of residual error analysis based Mathematica 10.0 package BVPh 2.0 interactions in the mass transfer analysis. The effect of various physical parameters is studied on flow velocity, temperature profiles and heat transfer rates are also analyzed.

The following conclusions are drawn from the present study.

- The influence of mass transfer parameter S, Hartman number M and shrinking parameter λ are similar trend in the velocity profile.

- The increase in mass transfer makes the temperature profile to converge faster to its free stream values.
- An increase in nanoparticle volume fraction $(\phi)$ decreases the velocity of the nanofluid. Furthermore the temperature and heat transfer rate are enhanced for larger values of Biot number.
- There is a decrease in temperature profile for larger values of shrinking parameter λ, and mass transfer parameter S.

**Acknowledgements**

The authors express their sincere thanks to the reviewers for their valuable comments and suggestions that helped us to improved the paper.

**References**

[1] Choi, S. U. S, (1995): Enhancing thermal conductivity of fluids with nanoparticles, in Proc. ASME, Int. Mechanical Engineering Congress and Exposition ASME, 66, 99-105.

[2] Das, S. K., Choi, S. U. S and Patel, H. Em (2006): Heat transfer in nanofluids-a review, Heat Transfer Engineering, **27,** 3–19.

[3] Wang, X. Q and Majumdar, A. S, (2007): Heat transfer characteristics of nanofluids -a review, Int. J. Thermal Sci., **46**, 1-19.

[4] Wang, X. Q. and Mujumdar, A. S, (2008): A review on nanofluids-Part I: Theoretical and numerical investigations, Brazilian J. Chem. Eng., **25**, 613–630.

[5] Sparrow, E. M., & Cess, R. D. (1978): Radiation heat transfer. Series in Thermal and Fluids Engineering, New York: McGraw-Hill.

[6] Kakac, S., and Pramuanjaroenkij, A., (2009): Review of convective heat transfer enhancement with nanofluids, Int. J. Heat Mass Transfer, **52**, 3187–3196.

[7] Niu, J., Fu, C., & Tan, W. (2012): Slip-flow and heat transfer of a non-Newtonian nanofluid in amicrotube, PLoS One, 7(5), e37274.

[8] Xu, H., Pop, I. and You, X.C., (2013): Flow and heat transfer in a nano-liquid film over an unsteady stretching surface, Int. J. Heat Mass Transfer, **60,** 646-665.

[9] Turkyilmazoglu, M., (2014): Nanofluid flow and heat transfer due to a rotating disk, Computer. Fluids, **94**, 139–146.

[10] Sheikholeslami, M., Ellahi, R.,Ashorynejad, H.R., Donairry, G., and Hayat, T., (2014): Effects of heat transfer in flow of nanofluids over a permeable stretching wall in a porous medium, J. Comput. Theor. Nanosci., **11**, 486–496.

[11] Sheikholeslami, M., Hatami, M., and Ganji, D.D., (2014): Nanofluid flow and heat transfer in a rotating system in the presence of a magnetic field, J. Mol. Liq., **190,** 112– 120.

[12] Sheikholeslami, M., Ganji, D.D., M.Y. Javed, M.Y., and Ellahi, R., (2015): Effect of thermal radiation on magneto hydrodynamic nanofluid flow and heat transfer by means of two phase model, J. Magn. Magn.Mater., **374**, 36–43.

[13] Ramzan, M., (2015): Influence of Newtonian heating on three dimensional MHD flow of couple stress nanofluid with viscous dissipation and Joule heating, PLoS One, **10 (4)**, 1246-1299.

[14] Hayat,T., Imtiaz, M., and Alsaedi, A., (2015): MHD 3D flow of nanofluid in presence of convective conditions, Journal of Molecular Liquids, **212**, 203-208.

[15] Hady,F. M., Ibrahim, I. S., Abdel-Gaied S. M., and Eid, M. R., (2012): Radiation effect on viscous flow of a nanofluid and heat transfer over a nonlinearly stretching sheet, Nanoscale Research Letters,**7**, 229-232.

[16] Nadeem, S., and Hag, R.U., (2013): Effect of thermal radiation for magnetohydrody namic boundary layer flow of a nanofluid past a stretching sheet with convective boundary conditions, Journal of Computational and Theoretical Nanoscience,**11**, 32-40.

[17] Nadeem, S., & Ul Haq, R. (2012): MHD boundary layer flow of a nanofluid passed through a porous shrinking sheet with thermal radiation, J of Aerospace Engg, 28(2), 04014061.

[18] Turkyilmazoglu, M., and Pop, I., (2013): Heat and mass transfer of unsteady natural convection flow of some nanofluids past a vertical infinite flat plate with radiation effect, Int. J. Heat Mass Transf. **59,** 167–171.

[19] Hsiao, K.L., (2014): Nanofluid flow with multimedia physical features for conjugate mixed convection and radiation, Comput. Fluids, **104**, 1–8.

[20] Kahar, A., Kandasamy, R.R. and Muhaimin, I., (2013): Scaling group transformation for boundary-layer flow of a nanofluid past a porous vertical stretching surface in presence of chemical reaction with heat radiation. Computers & Fluids, **52**, 15–21.

[21] S. J. Liao., (2012): Homotopy analysis method in nonlinear differential equatuions, Higher Education Press, Beijing.

[22] A. Rauf, S.A. Shehzad, T. Hayat, M.A. Meraj, and A. Alsaedi., (2017): MHD stagnation point flow of micro nanofluid towards a shrinking sheet with convective and zero mass flux conditions, Bulletin of the Polish Academy of Sciences Technical Sciences, 65(2), 155-162.

[23] K. P. Priyadarsan, M. K. Nayak, and S. Panda, (2017): Heat Transfer Effects on MHD 3D-Flow of Nanofluid by a Shrinking Surface, American Journal of Heat and Mass Transfer, 4(2), 64-84.

[24] M.K. Nayak, Noreen Sher Akbar , V.S. Pandey , Zafar Hayat Khan, Dharmendra Tripathi, (2017): 3D free convective MHD flow of nanofluid over permeable linear stretching sheet with thermal radiation, Powder Technology 315, 205–215.

[25] Salem AM, Fathy R., ( 2010): Effect of thermal radiation on MHD mixed convective heat transfer adjacent to a vertical continuously stretching sheet in the presence of variable viscosity. J Korean Phys Soc, 57(6), 1401-1407.

[26] Raptis A., (1998): Radiation and free convection flow through a Porous medium. Int Commun Heat Mass Transfer, 25, 289-295.

[27] L. Zheng, J. Niu, X. Zhang, Y. Gao, (2012): MHD flow and heat transfer over a porous shrinking surface with velocity slip and temperature jump, Math. Comput. Model., 56, 133–144.